# MODELLING CRACK EXTENSION IN BIAXIALLY LOADED PANELS

I. SCHEIDER, I., M. SCHÖDEL, W. SCHÖNFELD & W. BROCKS
Institute for Material Research, GKSS Research Centre, D-21502 Geesthacht, Germany

ABSTRACT

Two approaches for simulating ductile crack extension, namely the CTOA criterion and the cohesive model, are investigated, compared and validated for cracks in thin aluminium panels. The respective parameters are identified by numerical simulations of fracture tests on compact tension type specimens. The models are validated by using the same parameters for predicting crack extension in specimens of other sizes and loading configurations, in particular centre cracked panels under uniaxial and biaxial tension. It is shown for both models, that a unique parameter set can be used for different types of specimens.

## 1 INTRODUCTION

Aluminium sheets have a wide range of application in modern transportation industries, underlying rigorous safety requirements. The concept of damage tolerant design demands that even a partly damaged structure may not fail in an unstable manner. Numerical simulation techniques based on fracture mechanics models are well suited to support these design concepts, as damage tolerance can neither be proven by costly experiments alone, nor does the determination of crack initiation give sufficient information about the residual strength of a structure in service. Though analytical methods have been developed, which are able to predict failure for 2D structures (see e.g. [1, 2]), numerical simulations are necessary and useful to verify analytical procedures or to solve complex 3D problems, which can hardly be assessed analytically. Several models for the simulation of ductile crack extension under monotonous loading have hence been developed during the last two decades. Two of them, which have attracted special attention for cracked metal sheets, are the crack tip opening angle (CTOA) criterion [3, 4] and the cohesive model [5, 6]. They will be applied for numerical simulations of crack extension in Al panels.

## 2 MECHANICAL TESTING

The aluminium-magnesium alloy Al 5083 H321, which is widely used in shipbuilding and automotive industry, is investigated in the present study. The rolled sheets are 3 mm thick. Different specimens have been manufactured from these sheets, namely flat tensile specimens with a width of 8 mm for the determination of the stress-strain curve and several fracture specimens of different sizes and geometries. All specimens were tested under quasi-static conditions.

The elastic properties, Young's modulus and Poisson's ratio, are $E$ = 68000 MPa and $\nu$ = 0.33, and the 0.2% proof stress is $R_{p0.2}$ = 243 MPa, taken as yield stress for the FE analyses. The elongation of the tensile specimens was measured by a conventional extensometer. The experimental data may be used for the determination of the stress-strain curve only up to maximum load, which was reached after an equivalent strain $\varepsilon_{eq}$ = 0.125. The corresponding tensile strength is $R_m$ = 346 MPa. The stress-strain curve has been extrapolated by a power law. It was found that anisotropy of the

rolled material is minor. Therefore isotropic von Mises plasticity has been used for all calculations.
Quasistatic fracture tests were performed on compact type specimens, centre cracked panels and cruciform specimens, see Table 1. All specimens are fatigue precracked. The centre-cracked cruciform specimens, see Figure 1a, are biaxially loaded, the biaxiality factor being $\lambda = F_y / F_x$

TABLE 1: Fracture specimens

| designation | specimen type | size | relative crack length $a/W$ |
|---|---|---|---|
| CT50 | C(T) | W = 50 mm | 0.5 |
| CT150 | C(T) | W = 150 mm | 0.5 |
| MT100 | M(T) | 2W = 100 mm | 0.3 |
| MT300 | M(T) | 2W = 300 mm | 0.2 |
| BIAX | cruciform | 2W = 300 mm | 0.2 |

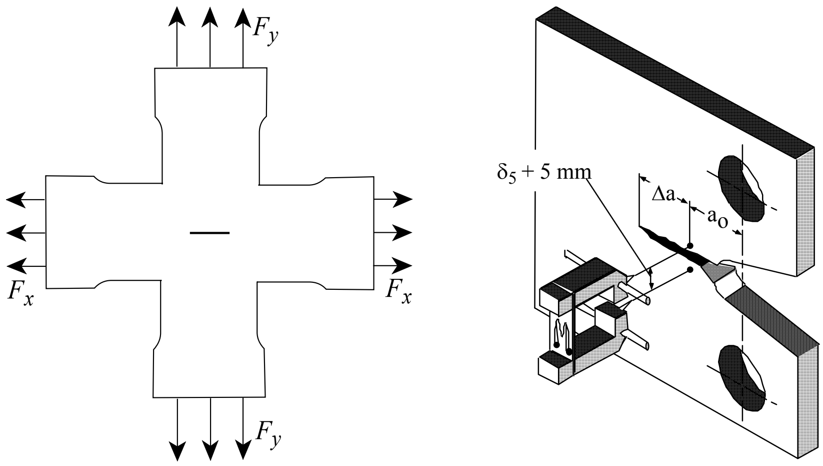


Figure 1. (a) Cruciform specimen under biaxial load, (b) clip gauge for the measurement of $\delta_5$

The specimens are equipped with clip gauges for measuring the load-line displacement or remote elongation, $V_{LL}$, and the crack tip opening displacement, CTOD $\delta_5$, see Figure 1b, and a camera for the determination of the crack length and CTOA. The remote elongation of the M(T) specimens is measured in a distance of $3 \times W$. Details of the experimental setup are described in [7].
The C(T) specimens are used for the determination of the respective material parameters, the M(T) and cruciform specimens for the validation of the models. For all specimens the load-displacement curves and the $\delta_5$ R-curves are examined.

## 3 NUMERICAL MODELS

The *crack tip opening angle*, CTOA, which has been introduced particularly for describing crack extension in metal sheets [3, 4], is used as characteristic parameter controlling crack extension, which is realised by a node release technique in the FE calculations. The underlying assumption is, that after initiation of crack extension no further crack-tip blunting occurs, and the deformation field at the crack tip is characterised by the opening angle, $\psi$, which remains constant for stationary crack extension [3, 4, 8].

$$\psi = \psi_{\mathrm{R}}(\Delta a)\,. \tag{1}$$

The advantage of this model is, that it requires only one parameter, which can be directly measured in fracture tests, see [7]. Within a defined range of application, the CTOA is closely related to the crack tip opening displacement (CTOD),

$$\psi \approx \frac{d\delta_5}{da}\,. \tag{2}$$

The idea of a *cohesive zone* at the crack tip goes back to considerations by Barenblatt. In modern applications, interface elements transferring cohesive stresses, $\boldsymbol{\sigma}$, which generally have one normal (mode I) and two tangential (mode II, III) components, are introduced between the continuum elements, which obey a separation law, $\boldsymbol{\sigma} = \boldsymbol{f}(\boldsymbol{\delta})$, where $\boldsymbol{\delta} = [\mathbf{u}]$ is the vector of the displacement jump between adjacent continuum elements. This cohesive law is purely phenomenological, and no possibilities exist for measuring it directly. It has obviously to be chosen in dependence on the respective micromechanical damage mechanism leading to fracture. In the present simulations, the following cohesive law was applied [9],

$$\sigma = \sigma_{\mathrm{c}} \begin{cases} 2\left(\dfrac{\delta}{\delta_1}\right) - \left(\dfrac{\delta}{\delta_1}\right)^3 & \text{for } \delta \le \delta_1 \\ 1 & \text{for } \delta_2 \le \delta \le \delta_{\mathrm{c}} \\ 2\left(\dfrac{\delta-\delta_2}{\delta_{\mathrm{c}}-\delta_2}\right)^3 - 3\left(\dfrac{\delta-\delta_2}{\delta_{\mathrm{c}}-\delta_2}\right)^2 & \text{for } \delta_2 \le \delta \le \delta_{\mathrm{c}} \end{cases}, \tag{3}$$

with the shape parameters $\delta_1 = 0.05\ \delta_c$, $\delta_2 = 0.50\ \delta_c$ and two material parameters, cohesive strength, $\sigma_c$. and critical separation, $\delta_c$. Instead of $\delta_c$. the work of separation, $\Gamma_{\mathrm{c}} \approx 0.73\sigma_{\mathrm{c}}\delta_{\mathrm{c}}$, represented by the area under the stress vs. separation curve, may be taken as material parameter. A general procedure for the determination of the parameters, $\sigma_c$ and $\Gamma_c$, for normal fracture, has been proposed in [10].

## 3 PARAMETER IDENTIFICATION

The C(T) tests have been used to determine the respective material parameters for CTOA and the cohesive model.

There is still no unique definition or measuring standard for CTOA. It was proposed in [7] to determine the angle from the opening displacements over a base length of 0.5 to 1.5 mm. For the first few millimetres of crack extension, the derivative of the $\delta_5$ R-curve, eq. (2), can be used, instead. The optically measured CTOA values as well as the derivative of the $\delta_5$ R-curve show that CTOA decreases after initiation and reaches a stationary value, $\psi_c$ [11]. A saturation value of 5°, which is reached after 8 mm crack extension, is taken for the simulations. As the optical data show significant scatter, a phenomenological fitting procedure based on the experimental load vs displacement curve and $\delta_5$ R-curve, is conveniently applied to identify $\psi_c$. The CTOA values in the simulations refer to a base length of 1 mm, over which the angle is calculated by the FE programme. The experimental (symbols) and the simulated (lines) load-displacement curves and $\delta_5$ R-curves achieved with this CTOA are shown in Fig. 2.

Following the procedure in [10], the parameters of the cohesive model should be in the range of $\Gamma_c \approx J_i = 7 \div 15$ kJ/m$^2$ and $\sigma_c \ge F_{\mathrm{frac}}/A_{\mathrm{frac}} = 484$ MPa. They have been determined by parameter fitting based on the experimental load vs displacement curve and $\delta_5$ R-curve of the C(T) specimens, yielding $\Gamma_c = 10$ kJ/m$^2$ and $\sigma_c = 560$ MPa. The resulting curves are also displayed in Fig. 2. The mesh dependence of the results has been studied by using different element lengths at the ligament (0.25 mm, 0.125 mm and 0.0625 mm), showing that below an element length of 0.125 mm the solution has converged. Therefore, all subsequent simulations have been performed with this element size.

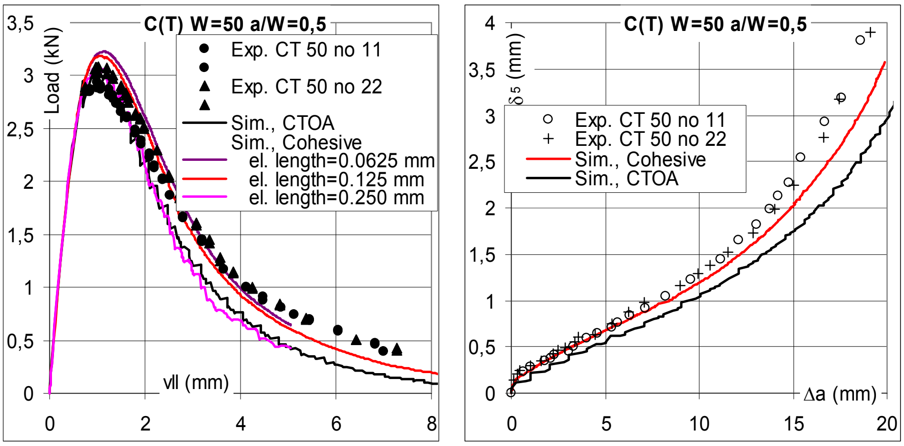


Figure 2: Experimental and simulated load-displacement curves (left) and $\delta_5$ R-curves (right), using CTOA criterion and cohesive model for the CT50 specimen. For the latter, results with different cohesive element lengths are shown in the load-displacement plot.

## 4 VERIFICATION

The difference in constraint between bend type and tension type specimens results in a problem of missing transferability of *J*-based R-curves. It is hence important, whether the above crack propagation models are able to overcome this problem and predict R-curves of different specimens with a unique set of parameters. Therefore, crack extension in two different M(T) specimens and a biaxially loaded cruciform specimen are simulated with the parameters determined above. Again, the load-deformation curve and the $\delta_5$ R-curve are evaluated. The results are shown in Figs. 3÷5. The cohesive model shows a very good agreement with the experimental curves, and the CTOA simulations are fairly good. A possible reason for the deviation of the CTOA simulations from the experimental curves for the M(T) specimens is the difference in the length of the transition zone to stationary crack growth, which is 8 mm for the C(T) and 10 mm for the M(T) specimens. Nevertheless, the maximum load, which is the most interesting quantity, is well predicted with the CTOA model in all cases, too.

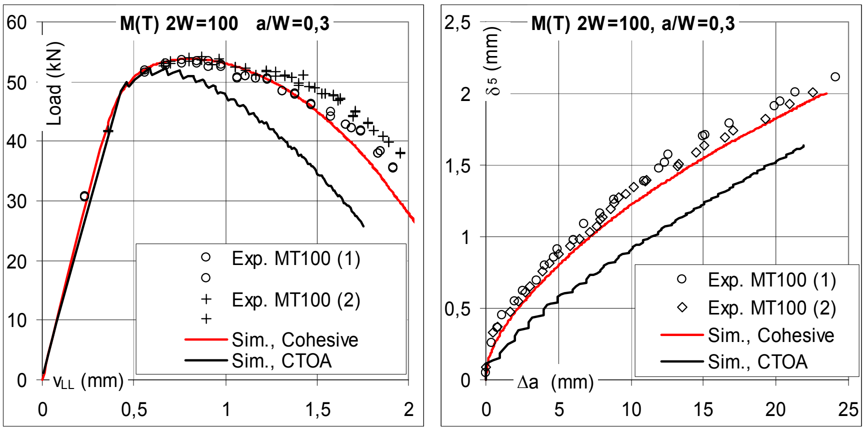


Figure 3: Experimental and simulated load-displacement curves (left) and $\delta_5$ R-curves (right), using CTOA criterion and cohesive model for the MT100 specimen.

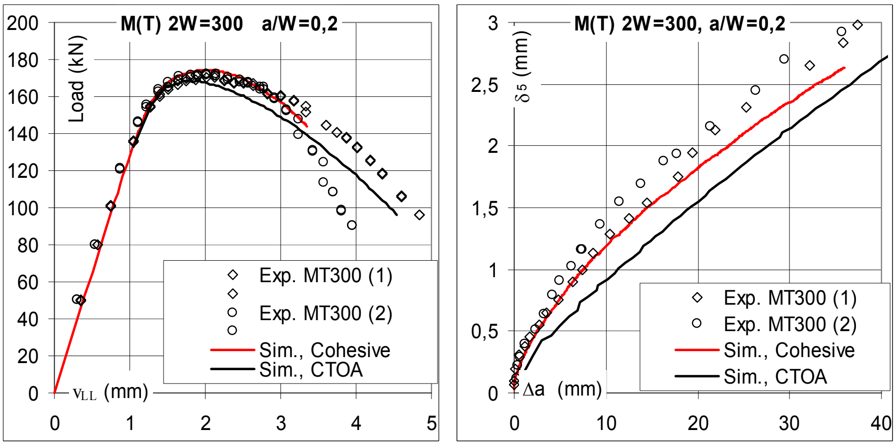


Figure 4: Experimental and simulated load-displacement curves (left) and $\delta_5$ R-curves (right), using CTOA criterion and cohesive model for the MT300 specimen.

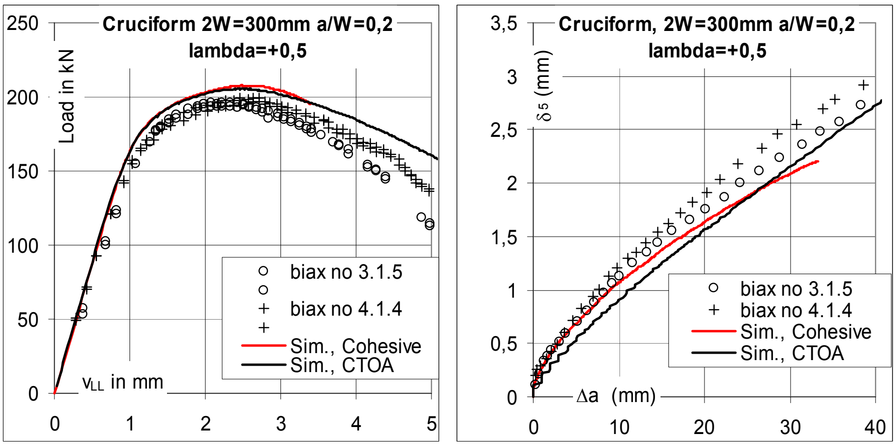


Figure 5: Experimental and simulated load-displacement curves (left) and $\delta_5$ R-curves (right), using CTOA criterion and cohesive model for the biaxially loaded cruciform specimens, $\lambda = 0.5$.

## 5 CONCLUSIONS

The numerical simulations showed that large crack extensions and the ultimate strength of thin-walled panels can be predicted by both the CTOA criterion and the cohesive model with good accuracy. For small specimens, where the transition region of crack extension is important for the overall behaviour, the variation of CTOA with crack extension, $\psi_R(\Delta a)$, must be taken into account. For larger specimens, where this range is only a small portion of the total crack extension, the assumption of constant CTOA leads to very good results. This has been confirmed by tests with C(T) specimens up to a width of $W = 1000$ mm, which are not shown here.

Despite the fact, that the results for the CTOA model are not as accurate as those for the cohesive model, the model has some promising advantages:

- The method is very robust and numerically stable;
- Larger elements can be used, which makes the FE model small and computation times short;
- A single parameter curve is sufficient for different constraint conditions and sizes;
- The $\psi_R(\Delta a)$ curve can be directly determined from tests;
- The method is not sensitive to uncertainties in the stress-strain curve.

Advantages of the cohesive model are

- The method yields very good results for structures with different size and constraint conditions;
- The two model parameters cohesive strength, $\sigma_c$. and separation energy, $\Gamma_c$, have some physical plausibility and can easily be determined by fitting of simulation results to experimental records;
- The cohesive model can not only be used for 2D thin walled, but also for thick or complex 3D structures;
- The presence of an initial crack is not essential for the cohesive model.

## 6 REFERENCES

[1] Schwalbe, K.-H., Zerbst, U., Kim, Y.-J., Brocks, W., Cornec, A., Heerens, J. and Amstutz, H.: EFAM ETM 97 - *The ETM Method for Assessing Crack-Like Defects in Engineering Structures.* GKSS Report GKSS/98/E/6, 1998.

[2] Ainsworth, R.A., Bannister, A.C. and Zerbst, U.: An overview on the SINTAP defect assessment procedure and its validation. *Int. J. Pres. Ves. & Piping* vol. **77**, 869-876, 2001.

[3] Dawicke, D.S., Sutton, M.A., Newman, J.C. Jr. and Bigelow, C.A.: Measurements and analysis of critical CTOA for thin-sheet aluminium alloy materials. In *Fracture Mechanics, 25$^{th}$ volume, ASTM STP 1220*, edited by Erdogan, F. and Hartranft, J., ASTM, Philadelphia, 358-379, 1995.

[4] O'Donoghue, P.E., Kanninen, M.F., Leung, C.P., Demofonti, G., and Venzi, S.: The development and validation of a dynamic fracture propagation model for gas transmission pipelines. *Int. J. Pres. Ves. & Piping* vol. **70,** 11-25, 1997.

[5] Needleman, A.: An analysis of decohesion along an imperfect interface. *Int. J. Fracture* vol. **42**, 21-40, 1990.

[6] Yuan, H., Lin, G. and Cornec, A.: Verification of a cohesive zone model for ductile fracture. *J. Eng. Mat. Techn.* vol. **118**, 192-200, 1996.

[7] Heerens, J. and Schödel, M.: On the determination of crack tip opening angle, CTOA, using light microscopy and $\delta_5$ measurement technique. *Eng. Fract. Mech.* vol. **70**, 417-426**,** 2003.

[8] Newman, J.C. Jr., James, M.A. and Zerbst, U.: A review of the CTOA/CTOD fracture criterion. *Eng. Fract. Mech.* vol. **70**, 371-385**,** 2003.

[9] Scheider, I., and Brocks, W.: Simulation of cup-cone fracture in round bars using the cohesive zone model. *Eng. Fract. Mech.* vol. **70**, 1943-1961, 2003.

[10] Cornec, A., Scheider, I., and Schwalbe, K.-H.: On the practical application of the cohesive model. *Eng. Fract. Mech.* vol. **70,** 1963-1987, 2003.

[11] Brocks, W., Negre, P., Scheider, I., Schödel, M., Steglich, D. and Zerbst, U.: Structural integrity assessment by models of ductile crack extension in sheet metal. *Steel Research International* vol. **75** (8), 504-513, 2003.